Innovative Instrumentation and Analysis of the Temperature Measurement for High Temperature Gasification

Type of Report: Semi-Annual Technical Report

Reporting Period Starting Date: 10/1/2003
Reporting Period End Date: 3/31/2004

Principal Author(s): Dr. Seong W. Lee

Date Report was issued: April 2004

DOE Award Number: DE-PS26-02NT41681

Name and Address of Submitting Organization:
Morgan State University
School of Engineering
5200 Perring Parkway
Baltimore, MD 21239

DISCLAIMER

This report was prepared as an account of work sponsored by an agency of the United States Government. Neither the United States Government nor any agency thereof, nor any of their employees, makes any warranty, express or implies, or assumes any legal liability or responsibility for the accuracy, completeness, or usefulness of any information, apparatus, product, or process disclosed, or represents that its use would not infringe privately owned rights. Reference herein to any specific commercial product, process, or service by trade name, trademark, manufacturer, or otherwise does not necessarily constitute or imply its endorsement, recommendation, or favoring by the United States Government or any agency thereof. The views and opinions of authors expressed herein do not necessarily state or reflect those of the United States Government or any agency thereof.

ABSTRACT

The systematic tests of the gasifier simulator were conducted in this reporting period. In the systematic test, two (2) factors were considered as the experimental parameters, including air injection rate and water injection rate. Each experimental factor had two (2) levels, respectively. A special water-feeding device was designed and installed to the gasifier simulator. Analysis of Variances (ANOVA) was applied to the results of the systematic tests. The ANOVA shows that the air injection rate did have the significant impact to the temperature measurement in the gasifier simulator. The ANOVA also shows that the water injection rate did not have the significant impact to the temperature measurements in the gasifier simulator. The ANOVA analysis also proves that the thermocouple assembly we proposed was immune to the moisture environment, the temperature measurement remained accurate in moisture environment.

Within this reporting period, the vibration application for cleaning purpose was explored. Both ultrasonic and sub-sonic vibrations were considered. A feasibility test was conducted to prove that the thermocouple vibration did not have the significant impact to the temperature measurements in the gasifier simulator. This feasibility test was a 2^2 factorial design. Two factors including temperature levels and motor speeds were set to two levels respectively. The sub-sonic vibration tests were applied to the thermocouple to remove the concrete cover layer (used to simulate the solid condensate in gasifiers) on the thermocouple tip. It was found that both frequency and amplitude had significant impacts on removal performance of the concrete cover layer.

TABLE OF CONTENTS

LIST OF GRAPIHICAL MATERIALS

1. INTRODUCTION

Gasification is a process that uses heat, pressure, and steam to convert materials directly into a gas composed primarily of carbon monoxide and hydrogen. Gasification technologies differ in many aspects but rely on four key engineering factors [1]:

1. Gasification reactor atmosphere (level of oxygen or air content).
2. Reactor design.
3. Internal and external heating.
4. Operating temperature.

Typical raw materials used in gasification are coal, petroleum-based materials, and organic materials. The feedstock is prepared and fed, in either dry or slurried form, into a sealed reactor chamber called a gasifier. The feedstock is subjected to high heat, pressure, and either an oxygen-rich or oxygen-starved environment within the gasifier. Most commercial gasification technologies do not use oxygen. All required an energy source to generate heat and begin processing.

There are three primary products from gasification:

- Hydrocarbon gases (also called syngas).
- Hydrocarbon liquids (oils).
- Char (carbon black and ash).

The syngas is primarily carbon monoxide and hydrogen (more than 85 percent by volume) and smaller quantities of carbon dioxide and methane [1]. The syngas can be used as a fuel to generate electricity or steam, or as a basic chemical building block for a multitude of uses.

When mixed with air, syngas can be used in gasoline or diesel engines with few modifications to the engine.

Because of the harsh operation environment, many problems occur in the normal operation. A lot of research has been conducted in the gasification process. In order to reduce the research cost, a simulator is normally used for the gasification research [2].

Within this research period, the vibration application for cleaning purpose is explored. Both ultrasonic and sub-sonic vibration were considered. The ultrasonic vibration frequency is above 20khz. The sub-sonic vibration frequency is below 20khz. According to the literature survey, ultrasonic vibration clean the object based on the high vibration strength, while the sub-sonic vibration clean the object based on the harmony vibration.

The design of experiment is heavily used in the research. Experimental design methods have found broad applications in many disciplines [3,4]. In fact, experimentation can be viewed as part of the scientific process and as one of the ways to reveal how systems or processes work. Generally, the researchers could learn through a series of activities in which they make conjectures about a process, perform experiments to generate data from the process, and then use the information from the experiments to establish new conjectures, which lead to new experiments, and so on.

Experimental design is a critically important tool in the engineering world for improving the performance of a manufacturing process [3]. It also has extensive application in the development of new processes. The applications of experimental design techniques early in process development can result in: improved process yields, reduced variability and closer conformance to nominal or target requirements, reduced developmental time, and reduced overall cost.

Experimental design methods also play a major role in engineering design activities, where new products are developed and existing ones are improved. Some applications of experimental design in engineering design/process include:

1. Evaluation and comparison of basic design configurations.
2. Evaluation of material alternatives.
3. Selection of design parameters so that the product will work well under a wide variety of field conditions, that is, so that the product is robust.
4. Determination of key product design parameters that impact product performance.

The use of experimental design in these areas can result in products that are easier to manufacture. The use of experimental design in these areas can also result in products that have enhanced field performance and reliability, lower product cost, excellent product quality and shorter product design/development time.

Robust design is Dr. Taguchi's approach for determining the optimum configuration of design parameters for performance [4], quality, and cost. This method is to improve the implementation of total quality control. It is based on the design of experiments to provide near optimal quality characteristics for a specific objective. This method is often demeaned by academia for technical deficiencies, which can be improved by using response surface methodology. In the research, the design of experiments was used to conduct the ANOVA analysis and factorial design.

2. EXECUTIVE SUMMARY

Continuing with the pre-systematic tests of the gasifier simulator, which was reported in the last semi-annual report, the systematic test of the gasifier simulator was conducted in this research period. In the systematic test, two (2) factors were considered as the experimental parameters, which were air injection rate and water injection rate. Each experimental factor had two (2) levels, respectively. A 2^2 factorial design was setup. With the gasifier simulator, the relatively low water injection rate was provided initially to simulate the moisture environment. However, some problems occurred when the water feeding system was initially setup. The water could not be fed to the gasifier smoothly. A special water-feeding device was designed and installed to the gasifier simulator.

Analysis of Variances (ANOVA) was applied to the results from systematic tests. The ANOVA shows that the air injection rate did have the significant impact to the temperature measurement in the gasifier simulator. The impact is believed to be caused by that the cold air injection changed the heat balance in the simulator. The ANOVA also shows that the water injection rate did not have the significant impact to the temperature measurement in the gasifier simulator. With the small amount of water feeding to the simulator, the temperature measurement in the simulator was very much the same, instead of large variance comparing to that without water injection. The ANOVA analysis also proved that the proposed thermocouple assembly was immune to the moisture environment, the temperature measurement remained accurate in moisture environment.

Within this research period, the vibration application for cleaning purpose was explored. Both ultrasonic and sub-sonic vibration were considered for this research application. The ultrasonic vibration frequency is above 20khz. The sub-sonic vibration frequency is below 20khz. According to the literature survey, ultrasonic vibration clean the object based on the high vibration strength, while the sub-sonic vibration clean the object based on the harmony vibration. Because of the harmony vibration impact, the thermocouple vibration test was conducted to first determine the natural frequency of the thermocouple solid cover, secondly, to determine the removal impact of the harmony vibration. Before the systematic test of the thermocouple vibration, the feasibility test of the thermocouple vibration was conducted to prove that the vibration would not have the significant impacts to the temperature measurements in the gasifier simulator.

The 2^2 factorial design was set to study the impact of the vibration to temperature measurement. The two factors, which were temperature levels and motor speed levels, were set to two levels respectively. Motor speeds were set to be two levels, which were 3000 rpm and 6000 rpm, respectively. These two motor speeds corresponded to 50 HZ and 100 HZ respectively. Three (3) temperature readings were recorded when the temperature approached stable temperature.

The vibration was created by using a high-speed motor with an unbalanced object at the motor shaft. The unbalanced object created the vibration at the frequency that is identical to the motor rotating frequency. The motor was fixed to the thermocouple flange by a clamp. The connection between the thermocouple and the gasifier simulator was set to be flexible by installing 4-5 pieces of soft gaskets between the flanges. From the ANOVA, it was found that the vibration had no significant impact to the temperature measurements for any temperature levels in the gasifier simulator no matter what temperature level was. The interaction between the

vibration and temperature levels was also not significant. So it is believed that thermocouple vibration had no significant impact to the temperature measurements in the gasifier simulator.

A layer of concrete was attached to the thermocouple tip to simulate the solid condensate accumulation. The sub-sonic vibration tests were applied to the thermocouple to remove the concrete cover layer on the thermocouple tip. The sub-sonic vibration tests were conducted in a fashion of a 3^3 factorial design. It was found that both frequency and amplitude had significant impacts on the concrete cover layer elimination.

3. EXPERIMENTAL

3.1. Gasifier Simulator Systematic Experiment

3.1.1 Gasifier Simulator Systematic Experiment Setup

The experimental facilities used in this period were discussed in previous reports [5, 6]. Based on the preliminary systematic test results, the humidity environment shall be created in the gasifier simulator during this reporting period. However, introducing water into the gasifier simulator was one of the challenges because of the unpredictable and unstable pressure inside the simulator. Various modifications were made to accurately introduce constant water flow rate to the hot environment inside the simulator.

Initially, water was introduced through the simulator's exhaust pipe, as droplets. These droplets immediately turned into steam, as soon as it was introduced into the gasifier simulator. But later on, it was realized that this was not an accurate way to feed the water. Thus, the desired flow was never accomplished. Since the water was introduced at the exhaust pipe, where the gas exiting was hot, the pressure inside the simulator was relatively higher, so the water might not flow from the leading pipe to the exhaust pipe. And even if it flows, it would immediately exit gasifier simulator because of the carrying effect of the flowing hot air at the exhaust pipe. Thus, this necessitated some modification.

At first, it was thought that the problem was pressure changes in flowing water, so the water flow pressure was maintained at a constant by making the elevated head constant. This was accomplished by introducing a small-elevated reservoir with two outlets one at the top and the other at the bottom; and the water level was maintained at the position of the top outlet. This top outlet served as the over flow from the reservoir, and the bottom outlet served as an outlet

leading to the simulator. One inlet pipe introduced water into the reservoir at a flowrate between the two outlet flowrates which ensured that the pressure head was maintained at a constant level.

This approach could not solve the problem, since the flow desired was not introduced to the gasifier, even after changing the positions of inlet to the simulator. Thus, a third modification was applied. This modification, involved introducing water through the pipe delivering the air to the simulator. This pipe was located at the bottom of the gasifier simulator. To accomplish this, a calibrated tube, holding a certain amount of water, was incorporated to the system. This calibrated tube had an outlet inside the air delivery pipe. This outlet dripped water to a droplet distributor (a porous material, for this case a sponge that was placed in the air delivery pipe). This was done to ensure the accuracy of the water injection rate, which was critical to the gasifier simulator systematic tests.

The reason for introducing the sponge was to ensure that the air flowing into the system would have a certain amount of moisture content which would then turn into the vapor in the simulator. The air could collect this moisture from the dump sponge, which was constantly fed by dripping water. The dump sponge was designed to have a large contacting surface to the airflow in the pipe and in turn, air was moistened when passing through the dump material. The other advantage of having a porous material (sponge) was to reduce the possibility of air flowing through the calibrated cylinder outlet, creating a negative pressure against the water flow.

The pictorial view of the gasifier simulator test facility with the water introducing system is shown in Figure 1. The schematic diagram of the specially designed water introducing system is shown in Figure 2.

The calibrating process of the water introducing system was conducted by measuring the water flow rate through the pipe at a given time. This process determined how much of the water

injection rate was represented by one-centimeter drop. The details of the calibration data are shown in Table 1.

Figure 1. The Pictorial View of the Gasifier Simulator Test Facility
With the Water Introducing System

Table 1. Calibration Data for Water Measuring Tube of the Water Introducing System

Test # 1	Initial Reading (cm)	Final # Reading (cm)	Water Amount (ml)	Final Reading to Initial Reading (cm)	1cm/ml
1	20	82	20	62	0.323
2	7	42.5	10	35.5	0.282
3	43	75.5	10	32.5	0.308
4	3	38	10	35	0.286
5	38	70.5	10	32.5	0.308
				Average =	0.3014
Thus 1 cm drop will represent 0.3014ml.					

Figure 2. The Schematic Diagram of the Water Introducing System

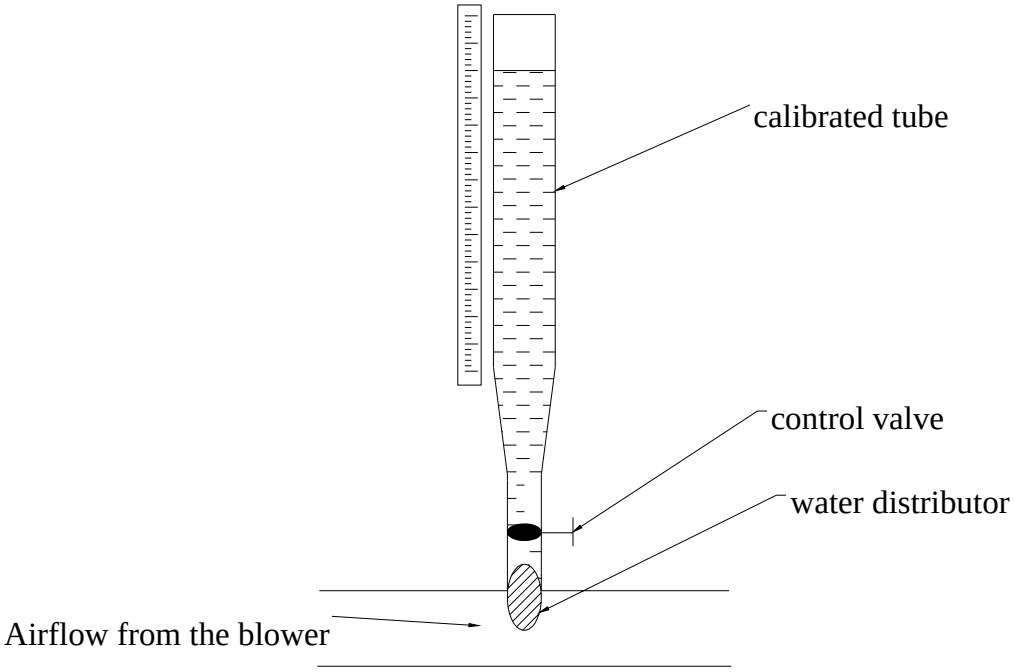

3.1.2 Gasifier Simulator Systematic Experimental Design and Procedure

The systematic test matrix is shown in Table 2. Two factors - air injection rate and water introducing rate, were considered to be significant factors to the gasifier temperature measurements.

Table 2. Systematic Test Matrix with Two Factors

Flow Rates Levels	Air Injection Flow Rate (m^3/sec)	Water Injection Flow Rate (ml/sec)
Low Level	0.0032	0.033
High Level	0.0044	0.05

The systematic experimental procedure at different air injection rates and different water injection rates is summarized as follows:

1) Assemble the gasifier simulator (hot model), blower, and manometer together.
2) Set the blower voltage at the highest position
3) Turn on the cooling water lines at the most amount
4) Setup and calibration of the thermal couples and record the ambient temperature
5) Turn on the heating coil
6) Operate the blower voltage regulator to obtain the different experimental conditions.
7) Record the experimental temperature data at every five (5) minutes
8) Check the system running at the stable state after one (1) hour
9) Turn off the heating coil
10) Record the cooling process temperature
11) Turn off the cooling water lines

3.2 Thermocouple Vibration (Ultrasonic and Sub-Sonic) Cleaning Application to the Gasification Process

One of the greatest problems for thermocouple to measure gasification temperature is the solid cover created by the melted gasifying materials condensating on the thermocouple. This cover is normally very difficult to be removed by a pressurized air purging system and/or other cleaning methods. The ultrasonic vibration method is considered to be one of the effective methods to remove the cover by its vibration strength and high frequency. However, sub-sonic vibration might also have good performance in removing the solid cover. Since the high cost of the ultrasonic application, the sub-sonic vibration was firstly applied by a high-speed motor

through a harmony vibration process of the solid cover. It is believed that the harmony vibration shall be able to remove the solid cover [7, 8].

3.2.1. Ultrasonic Vibration Application

After careful research in ultrasonic research, it was found that ultrasonic welding application could be applied to the thermocouple to remove the solid cover. The description of the ultrasonic welding application is described below.

Ultrasonic metal welding technology can be used for many different applications by appropriately utilizing its sound wave and high frequency mechanical energy characteristics [9,10]. The advantages of short-wave vibrations are excellent directional characteristics and high signal repeatability. This combination guarantees perfect traceability of faulty joints, determination of material characteristics and the thickness and structure of layers. Diagnostic equipment based on ultrasonic has become an indispensable and common device for medical applications.

Ultrasonic energy [11] is used to improve the structure of materials in metallurgy. The acoustic irradiation of molten mass leads to an improved degasification and finer grain structures during the hardening process. Thanks to the cavity flow of the energy-transmitting fluid and ultrasonic baths, high-frequency mechanical vibrations have a highly purifying effect. The pressure peaks (up to 1000 bar) not only assist in removing settlement surface particles as well as oil and grease, but also detach solid varnish coats for metal bodies with the help of low frequency vibrations.

When combined with the erosive media, ultrasonic drilling can be used as a finishing technique for shaping materials which are brittle and hard to work on such as glass, ceramics,

etc. Ultrasonic welding is a metallurgical process which utilizes many materials with different melting temperatures.

Ultrasonic metal welding technology has proven to be extremely successful in various applications, but above all, in electronics, the electrical industry, the automotive industry and in some other fields. The cost advantage and the quality improvements obtained by the use of this technology are considerable.

The unique effect of ultrasonic metal welding is low heat radiation with no melting mass. The process is determined by a few easily measurable welding parameters. This is why the welding process can easily be monitored and controlled electronically, which is a prerequisite for a safe process.

This document introduces the rather recent but nevertheless proven technology of ultrasonic metal welding: its basic principles, the required machinery, its components and the interaction of its different components, as well as possible applications and their limitations.

The different processes for joining metal parts can be systematically subdivided into different categories depending on their action principle. Their bond can be form-closed, frictional or positive-substance bond. Very often, it is not possible to make a clear distinction between closing shape and frictional bond, as some processes render a clear distinction between operating principles impossible.

A positive substance bond is mostly inseparable, and the bond takes place only by using additional material or consumables. The most frequent types of joints in this category are adhesive, soldered, brazed and welded joints. When welding materials, one has to distinguish between fusion welding and pressure welding.

Fusion welding leads to a welding of the pieces by applying heat at the point of connection, which fuses the pieces together and even, joins a material. After the hardening of the mixed components, a solid joint occurs [7.8]. Unlike fusion welding, pressure welding depends on the application of high pressures and/or high temperatures, resulting in a strong plastification and a local deformation of the pieces to be joined in the welding area so that a bond between both pieces is made. The energy required for the welding process is of a different kind for both types of procedure.

Proven energy sources here are gas, arc welding, light, electron or plasma beams. Ultrasonic welding belongs in the category of pressure welding and uses motion and kinetic energy for welding pieces together.

Depending on the kind of motion, a distinction in metal welding between cold-pressed welding, friction welding and ultrasonic welding can be made. All three procedures show a high similarity. Ultrasonic metal welding is a combination of cold-press welding and friction welding because of its mode of action.

Cold-press welding takes place at room temperature. By applying high pressures to both pieces the materials weld together. A strong material deformation at the welding zone accounts for the bond.

In the friction welder, one or both pieces rotate while they are pressed together. The frictional heat, which emanates together with the static pressure causes the bond between the pieces. The backpressure required for joining the pieces in comparison to cold-press-welding is drastically reduced because of the additional rotational energy. The matching of the surfaces promotes plastification and local deformation of the pieces being welded.

During ultrasonic metal welding, the rotational motion is replaced by mechanical linear vibrations. The welding surfaces are periodically scrubbed during the welding process. This further reduces the required welding pressure compared to friction welding, the final value being only about 1% of that required for cold-press welding.

3.2.2 Sub-sonic Vibration Application

Beside the ultrasonic vibration, sub-sonic vibration might also have good performance in removing the solid cover. Since the high cost of the ultrasonic application, the sub-sonic vibration was firstly applied using a high-speed motor with an unbalanced object at the motor shaft. It is believed that the harmony vibration shall be able to remove the solid condensate cover. The natural frequency of the similar material to the solid condensate cover at similar shape is around 10-100 HZ [12, 13]. Because of the harmony vibration impact, the thermocouple vibration test was conducted to first determine the natural frequency of the thermocouple solid condensate cover, secondly, to determine the removal impact of the sub-sonic vibration.

3.2.3 Feasibility Test of the Thermocouple Vibration

From the discussion in Section 3.2.1 and Section 3.2.2, both ultrasonic vibration and sub-sonic vibration might be able to remove the solid condensate cover. However, before start the systematic test of the vibration test, it is essential to prove that the vibration does not have the significant impacts to the temperature measurements in the gasifier simulator.

The 2^2 factorial design was set to study the impact of the vibration to temperature measurement. The two factors were temperature levels and motor speed levels, respectively. These two factors were set to two levels respectively. The test parameters and the experimental data are shown in Table 3. Motor speeds were set to be two levels, which were 3000 rpm and 6000 rpm, respectively. These two motor speeds corresponded to 50 HZ and 100 HZ respectively. Temperature levels were set to be low level (ambient level) and high level (around 1800 F). Three (3) temperature readings were recorded when the temperature approached steady state temperature.

Table 3. Test Parameters and Experimental Data
for the Feasibility Test of the Thermocouple Vibration

	Data Set 1 Temperature Reading 1 (F)	Data Set 2 Temperature Reading 2 (F)	Data Set 3 Temperature Reading 3 (F)
Motor Speed (3000 rpm) Frequency = 50 HZ	72.9	72.8	73
Motor Speed (3000 rpm) Frequency = 50 HZ	1754	1795	1731
Motor Speed (6000 rpm) Frequency = 100 HZ	72.8	73	73.1
Motor Speed (6000 rpm) Frequency = 100 HZ	1775	1795	1753

The vibration was created by a high-speed motor with an unbalanced object at the motor shaft. The unbalanced object created the vibration at the frequency that was identical to the motor rotating frequency. The schematic diagram of the vibration creation is shown in Figure 3. The motor was fixed to the thermocouple flange by a spring clamp. The connection between the thermocouple and the gasifier simulator was set to be flexible by installing 4 to 5 pieces of soft gaskets between the flanges. The flexible connection was designed not to limit the vibration created by the motor rotating. The actual image of the motor mounting to the thermocouple is shown in the Figures 4 and 5.

Figure 3. The Schematic Diagram of the Motor Vibration Creation

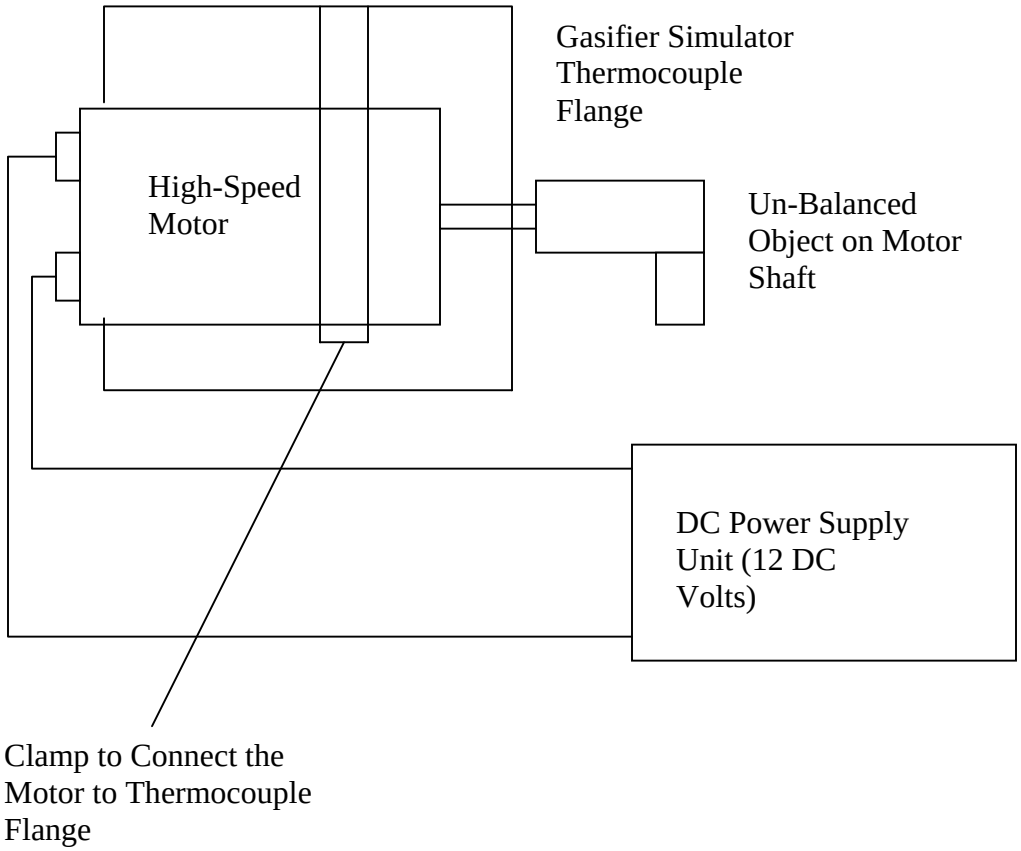

Figure 4. The Axis-View of the Motor Mounting

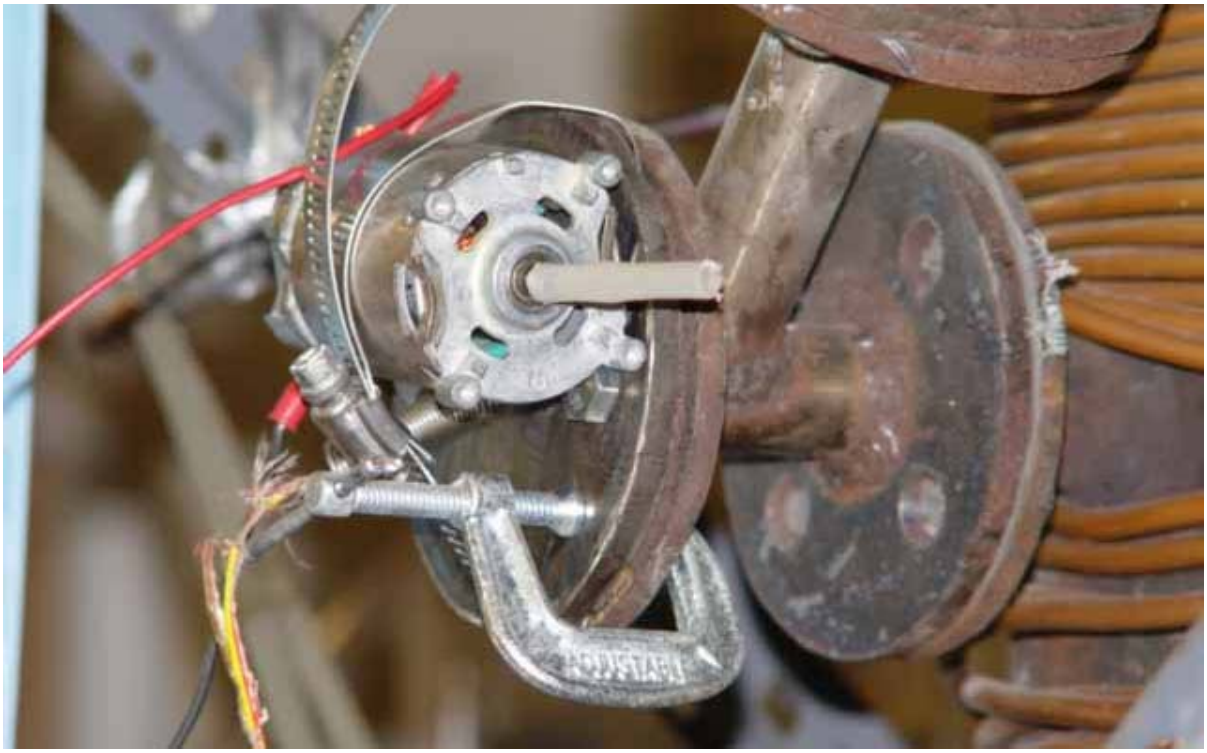

Figure 5. The Front-View of the Motor Mounting

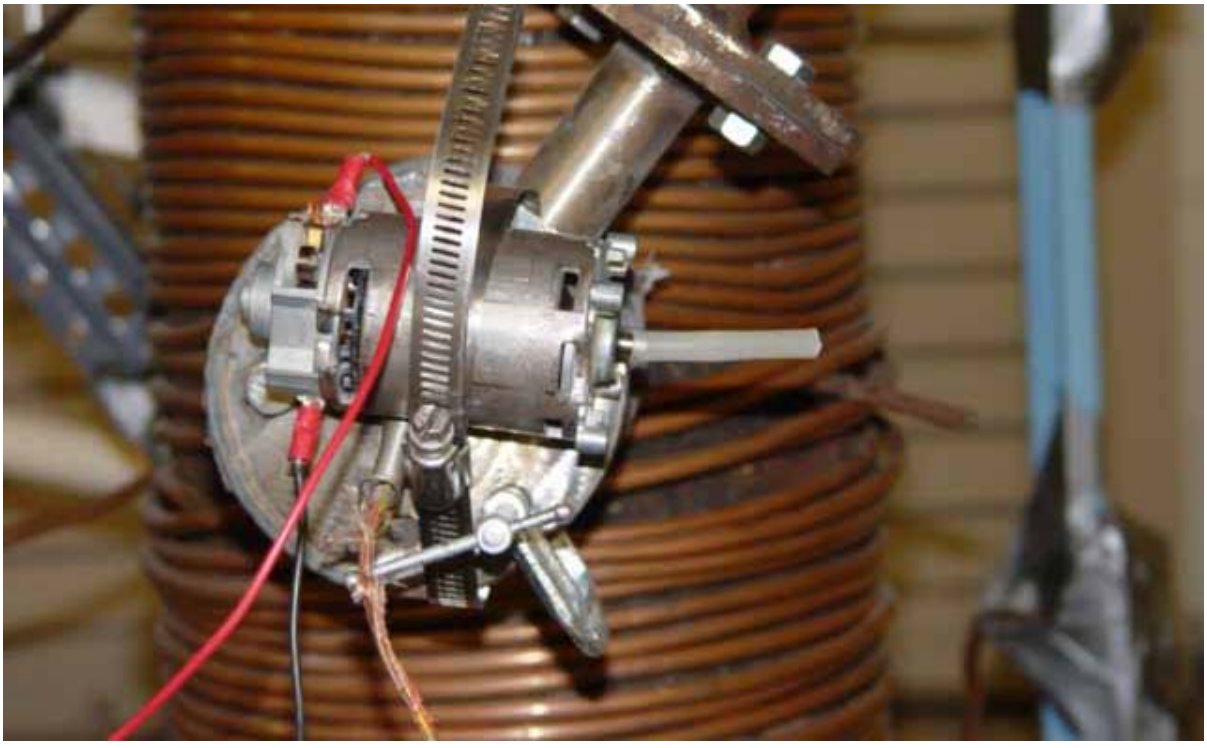

3.2.4 Sub-sonic Thermocouple Vibration Test

A concrete cover layer was attached to the thermocouple tip. This layer was to simulate the melted ash condensation at the thermocouple tip. The weight of attached concrete cover layer was 21.56 grams. The sub-sonic vibration tests were conducted at three different frequencies and three different vibration amplitudes; hence, nine (9) tests were conducted. The three (3) frequency levels were 100 Hz, 200 Hz, and 300 Hz, respectively. The three (3) vibration amplitude levels were approximate 0.1 mm, approximate 0.2 mm, and approximate 0.3 mm, respectively. The different vibration levels were created based on the different weight of the un-balanced mass on the motor. The motor used in the tests was Radio Shack' product, the maximum speed was 19800 RPM at 19.8 VDC and 0.89 Amps. The unbalanced weight was created by applying Goop Glue and special tape. The motor and thermocouple were connected by a spring clamp. The tightness of the connection was adjusted to get the maximum vibration amplitude at each frequency.

Table 4 shows the experimental setup and obtained data for the sub-sonic thermocouple vibration tests. These tests were conducted at ambient temperature environment (cold test environment). The purpose of these tests is to determine the removal performance of the thermocouple vibration to the attached concrete cover layer.

Table 4. Sub-sonic Thermocouple Vibration Test Setup and Data

	Vibration Frequency 100 Hz	Vibration Frequency 200 Hz	Vibration Frequency 300 Hz
Amplitude 0.1 mm appox.	0.323 grams	0.412 grams	0.498 grams
Amplitude 0.2 mm appox.	0.396 grams	0.478 grams	0.499 grams
Amplitude 0.3 mm appox.	0.456 grams	0.418 grams	0.599 grams

The pictorial view of the sub-sonic thermocouple vibration test facilities and motor/thermocouple connection in cold test environment is shown in Figures 6 and 7.

Figure 6. The Pictorial View of the Sub-sonic Vibration Test Facility

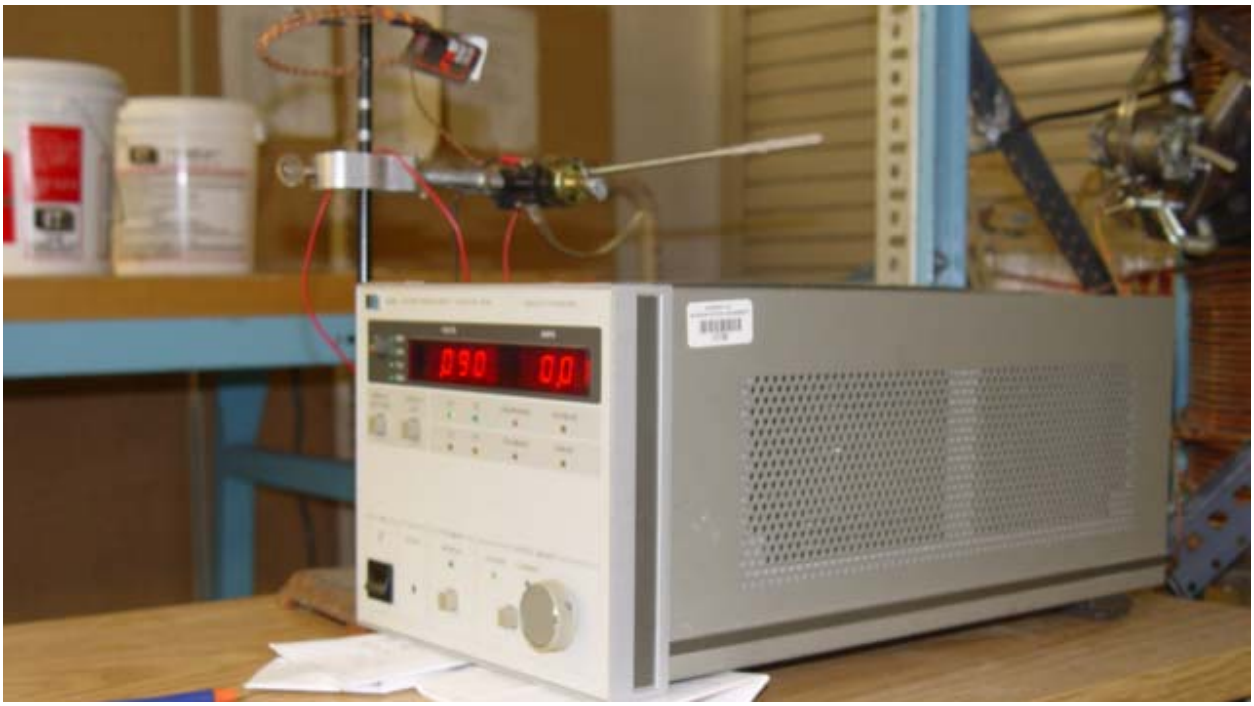

Figure 7. The Pictorial View of the Motor/Thermocouple Mounting

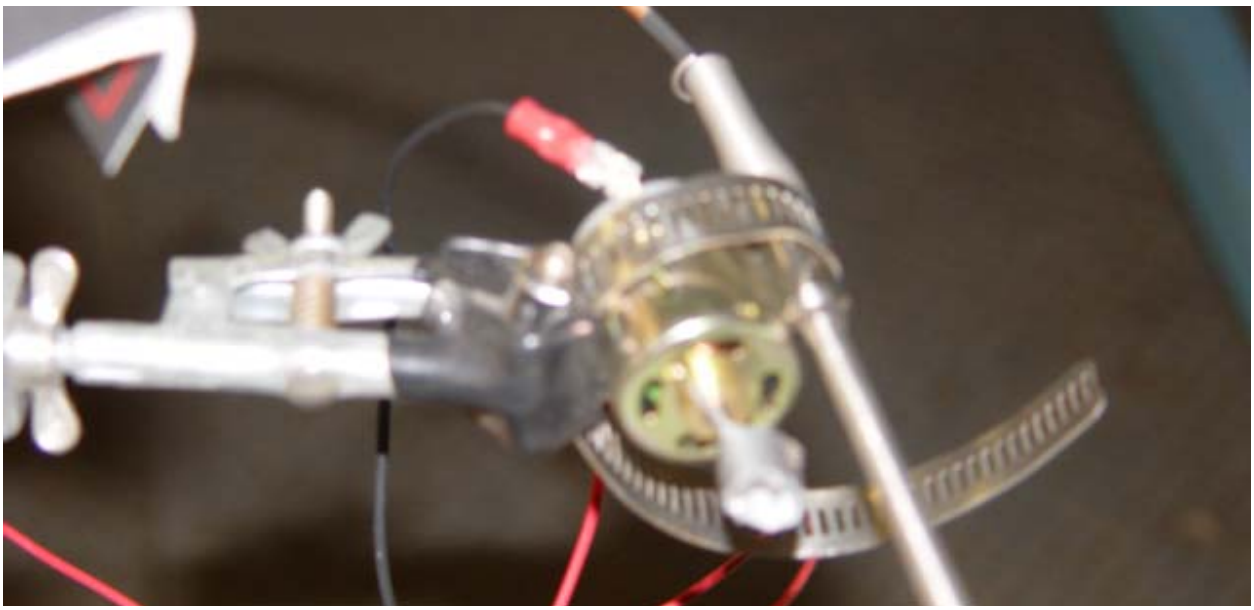

4. RESULTS AND DISCUSSION

4.1. Gasifier Simulator Systematic Experiment

4.1.1. Temperature Changes with the Different Air Injection Rates

The detailed experimental procedure and facilities are shown the previous section 3.1. A series of experiments were conducted to check the impact of the air injection rate on the temperature inside the simulated gasifier. With no air injection, the temperature heating up curve is shown in Figure 8. It took about 35 minutes to reach the steady state temperature as shown in Figure 8. The temperature at the top section of the gasifier simulator was about 1885 F 40 minutes after starting the experiment. And since then, the temperature reached the steady state temperature (around 1885±50 F).

Figure 8. Temperature Heating Up Curve without Air Injection

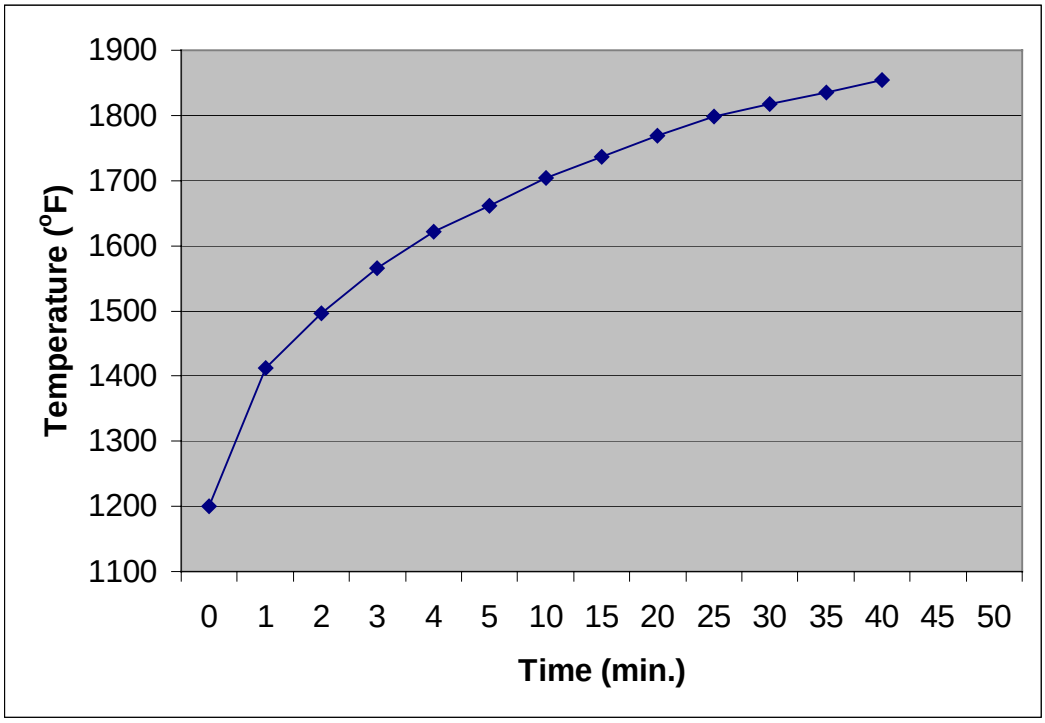

Figure 9. Temperature Cooling Down Curve without Air Injection

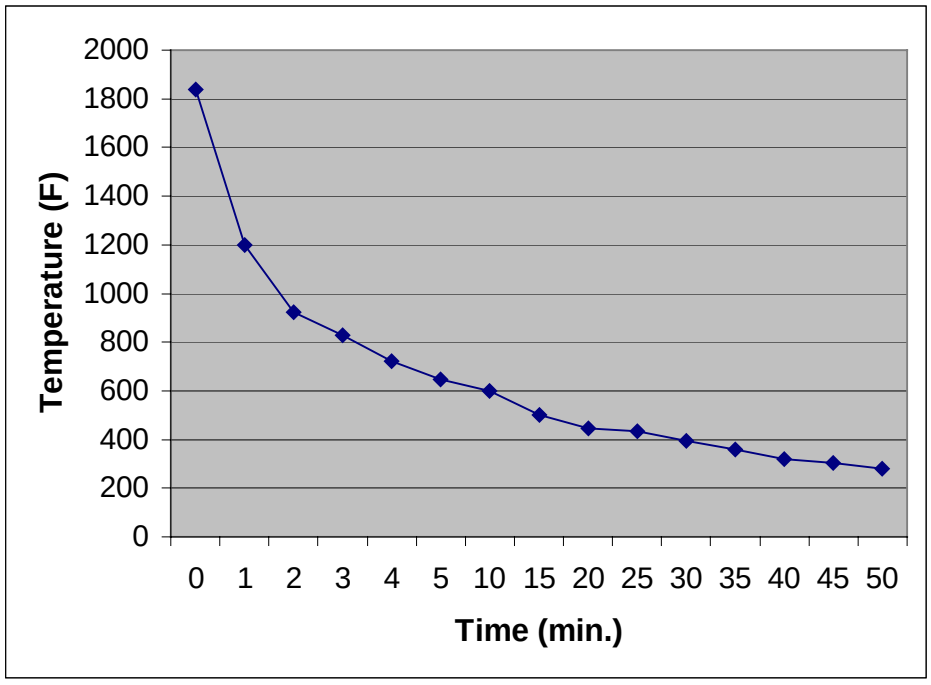

Figure 10. Temperature Heating Up Curve with Air Injection Rate of 0.0055 m^3/second

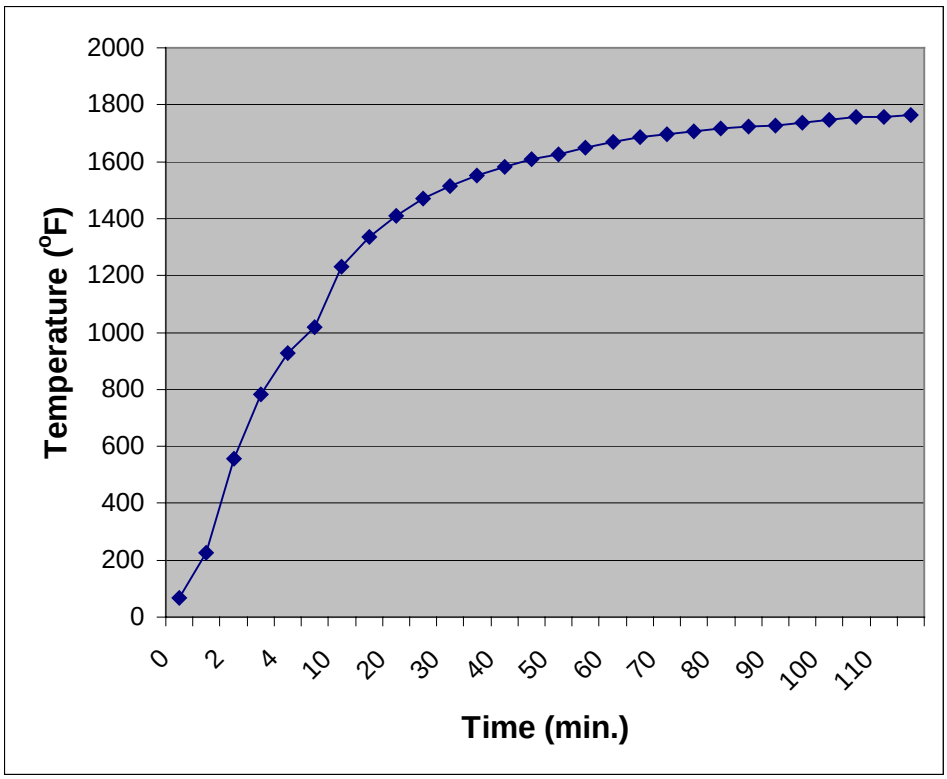

Figure 9 shows the temperature cooling down curve when no air injection was applied. For the first five (5) minutes, the temperature dropped almost 70%. And then, it began to decrease slowly.

Figures 10-13 show the temperature heating up curves with the different air injection rates. The steady state temperatures were normally reached after 40-50 minutes. For the first 20 minutes the temperature increased very fast. And then, it began to increase slowly. In order to record the temperature precisely, the temperature changes were recorded in one (1) minute intervals for the first five (5) minutes.

Figure 10 shows the temperature heating up curve when the air injection rate was 0.0055 m^3/second. The temperature change during the first five (5) minutes was from 60 F to 950 F at the rate of 180 F/minute. And then, the temperature heating up rate became 60 F/minute between the 5 to 25 minutes time period. After that, the temperature heating up rate was 10 F/minute until it became relatively stable at 1750F.

Figure 11 shows the temperature heating up curve when the air injection rate was 0.0067 m^3/second. The other operation factors remained the same of the test shown in Figure 10. It was found that the temperature heating up curve was quite similar to that at the air injection rate of 0.0055 m^3/second. The temperature heating up rate was less than that at the air injection rate of 0.0055 m^3/second. During the first five (5) minutes, the temperature heating up rate was 160 F/minute. Then, the temperature heating up rate changed to 35 F/minute during the time period of 5 to 25 minutes. After that, the temperature stabilized at 1600 F.

Figure 12 shows the temperature heating up curves when the air injection rate was 0.0078 m^3/second. During the first five (5) minutes, the temperature heating up rate was 150 F/minute.

This rate was less than those at the air injection rates of 0.0055 m^3/second and 0.0067 m^3/second. The steady state temperature was also lower than the steady state temperatures shown in Figures 8, 10 and 11.

Figure 12 also shows the temperature difference between the top section and median section of the gasifier simulator. During the first five (5) minutes, the temperature at the median section was higher than that of the top section. Then, the top section temperature was higher than that of the median section temperature after the first 5 minutes. At the steady state, the difference between the temperatures at the top and median sections was about 50 F.

Figure 13 shows the temperature heating up curve when the air injection rate was 0.0089 m^3/second. The temperature change rate for the first five (5) minutes was 110 F/minute. The steady state temperature was 600 F. The temperature of the top section was 150 F higher than that of the median section.

Figure 11. Temperature Heating Up Curve with Air Injection Rate of 0.0067 m^3/second

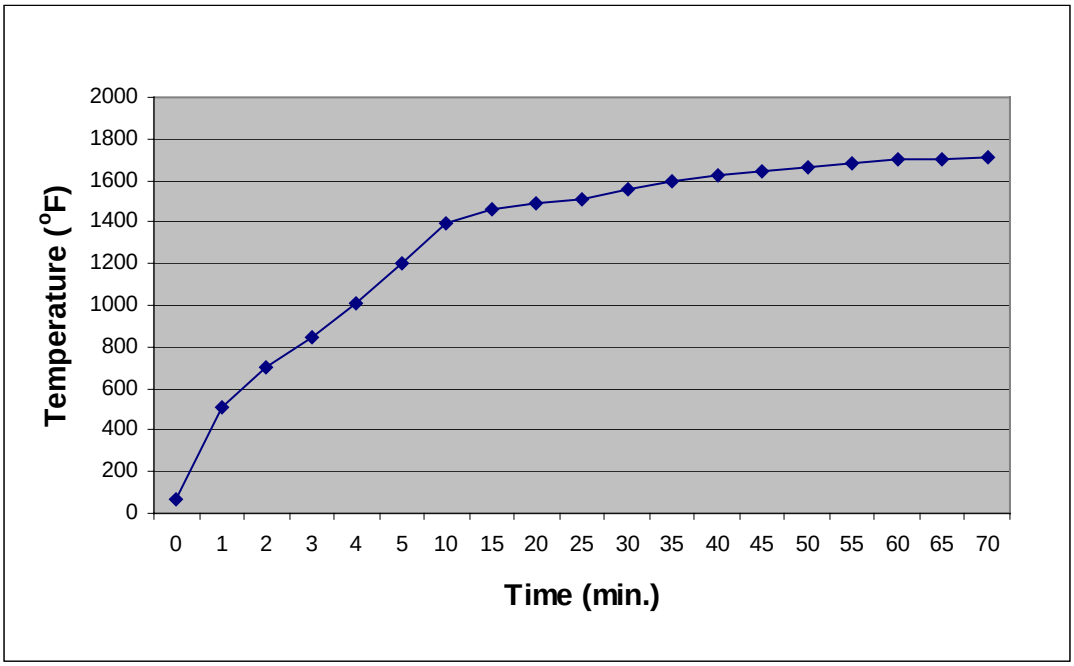

Figure 12. Temperature Heating Up Curve with Air Injection Rate of 0.0078 m^3/second

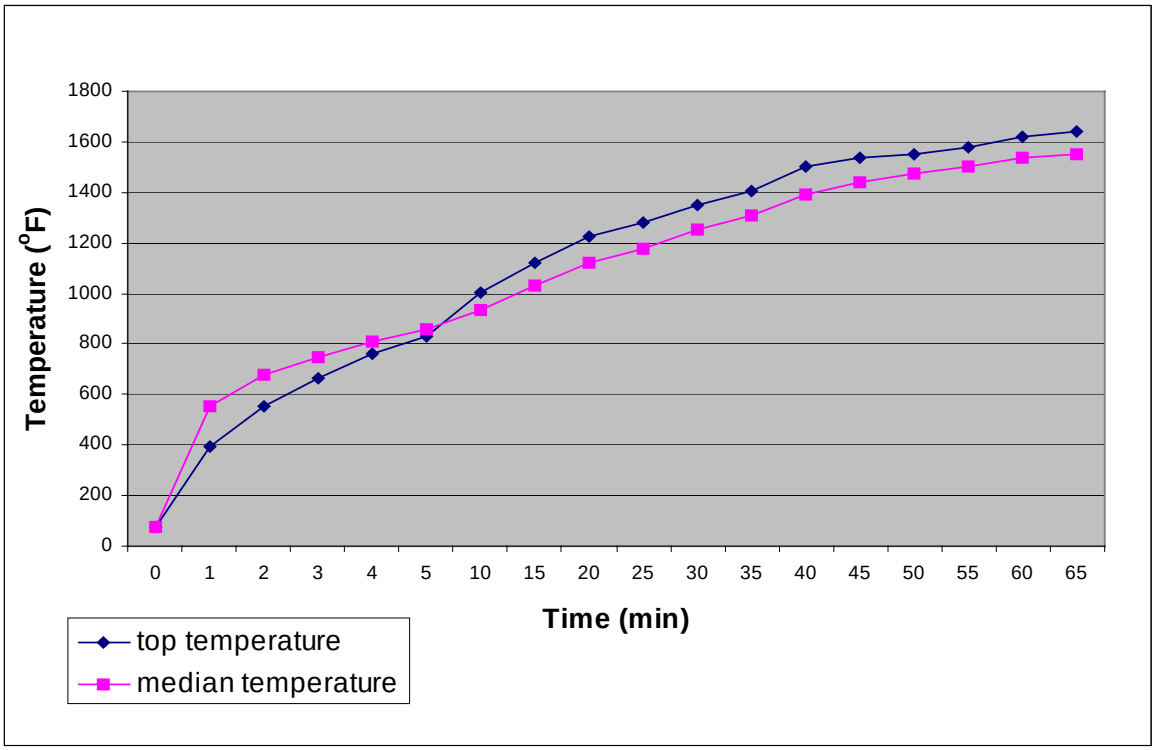

Figure 13. Temperature Heating Up with Air Injection Rate of 0.0089 m^3/second

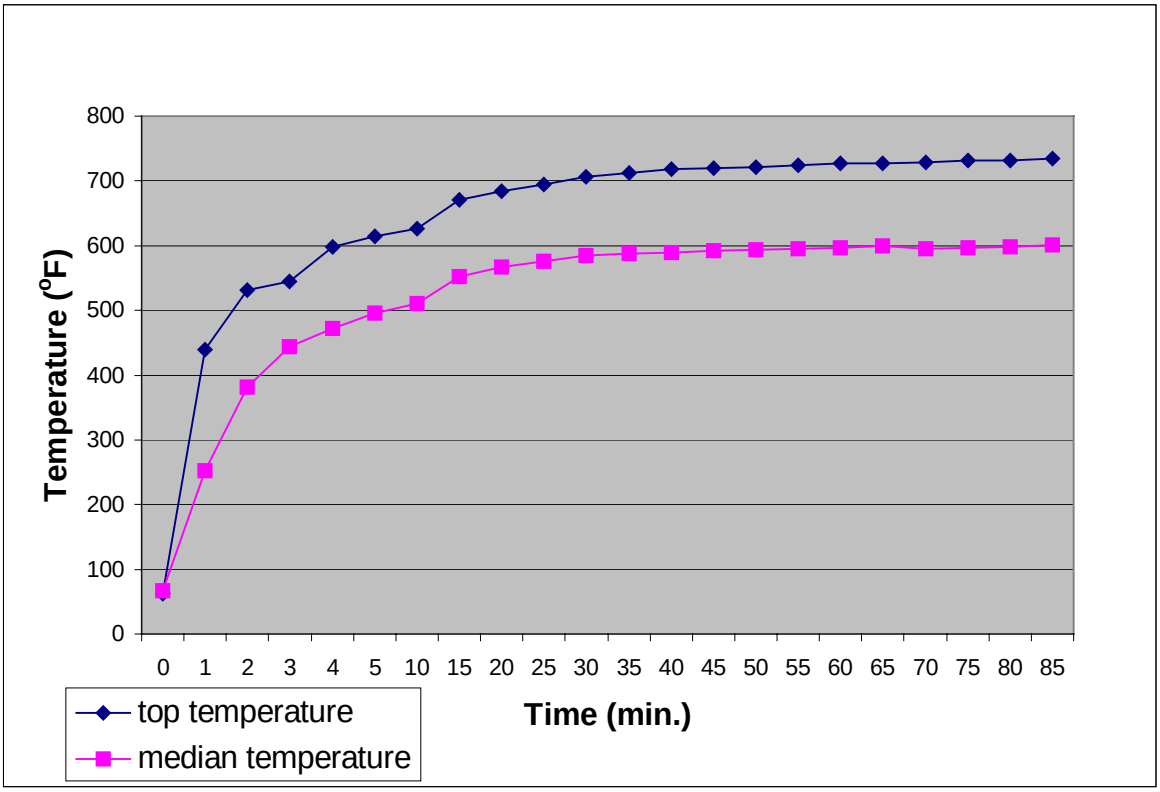

In overall, Figures 11, 12, and 13 indicates that temperature heating up rate was very fast but smooth throughout the heating up process. The steady state temperature was in the range from 750 F to 1750 F with respect to different air injection rates. When the air injection rate was 0.0089 m^3/second, the steady state temperature in gasifier simulator was too low in comparing to real gasifier operation conditions. So, the three air injection rates - 0.0055 m^3/second, 0.0067 m^3/second, and 0.0078 m^3/second, are suggested for the further experiments. Based on the discussion, it can also be concluded that the lower air injection rates are preferred for the systematic test in the gasifier simulator.

4.1.2 Temperature Changes with the Different Water Injection Rates

After installing the water introducing system, a series of tests were conducted to measure the temperature heating up rates inside the gasifier simulator. Two (2) factors were considered as the significant factors for temperature heating up rates. The two factors, including water injection rate and air injection rate, were set to two levels, respectively. The results were analyzed based on the statistical factorial design. The low level for the water injection rate was 0.0033 ml/second, and high level was 0.05 ml/second. The low level for the air injection rate was 0.0032 m^3/second, and high level was 0.0044 m^3/second. The test matrix is shown in Table 2. For the full factorial design, the 2^2 runs (total four cases) of the experiments were conducted. The results for the full factorial design of experiments are shown in Table 5. Figure 14 shows that the temperature heat up curve at four (4) different cases.

Table 5. Results for the Full Factorial Design of Experiments

Case No.	1	2	3	4
Water Injection Rate:	0.0033 ml/sec	0.05 ml/sec	0.05 ml/sec	0.0033ml/sec
Air Flow Rate:	0.0032 m^3/sec	0.0032 m^3/sec	0.044 m^3/sec	0.044 m^3/sec
Time min.	Temp. F	Temp. F	Temp. F	Temp. F
0	89.7	70	70	52.7
1	237.9	333	330	340
2	676.3	650	651	661
3	850.7	828	800	820
4	949.9	940	925	950
5	1016	1004	1004	1050
10	1175	1139	1130	1120
15	1268	1248	1228	1280
20	1335	1320	1315	1350
25	1388	1368	1368	1380
30	1425	1405	1415	1450
35	1466	1427	1429	1430
40	1507	1446	1436	1500
45	1536	1465	1456	1489
50	1563	1477	1467	1520
55	1582	1492	1489	1550
60	1596	1502	1505	1590.1
65	1614	1510	1515	1598.6
70	1623	1511	1501	1609
75	1631	1514	1504	1607
80	1646	1519	1509	1614
85	1657	1521	1511	1615
90	1669	1518	1508	1614
95	1676	1520	1510	
100	1680			
105	1688			
110	1693			
115	1698			

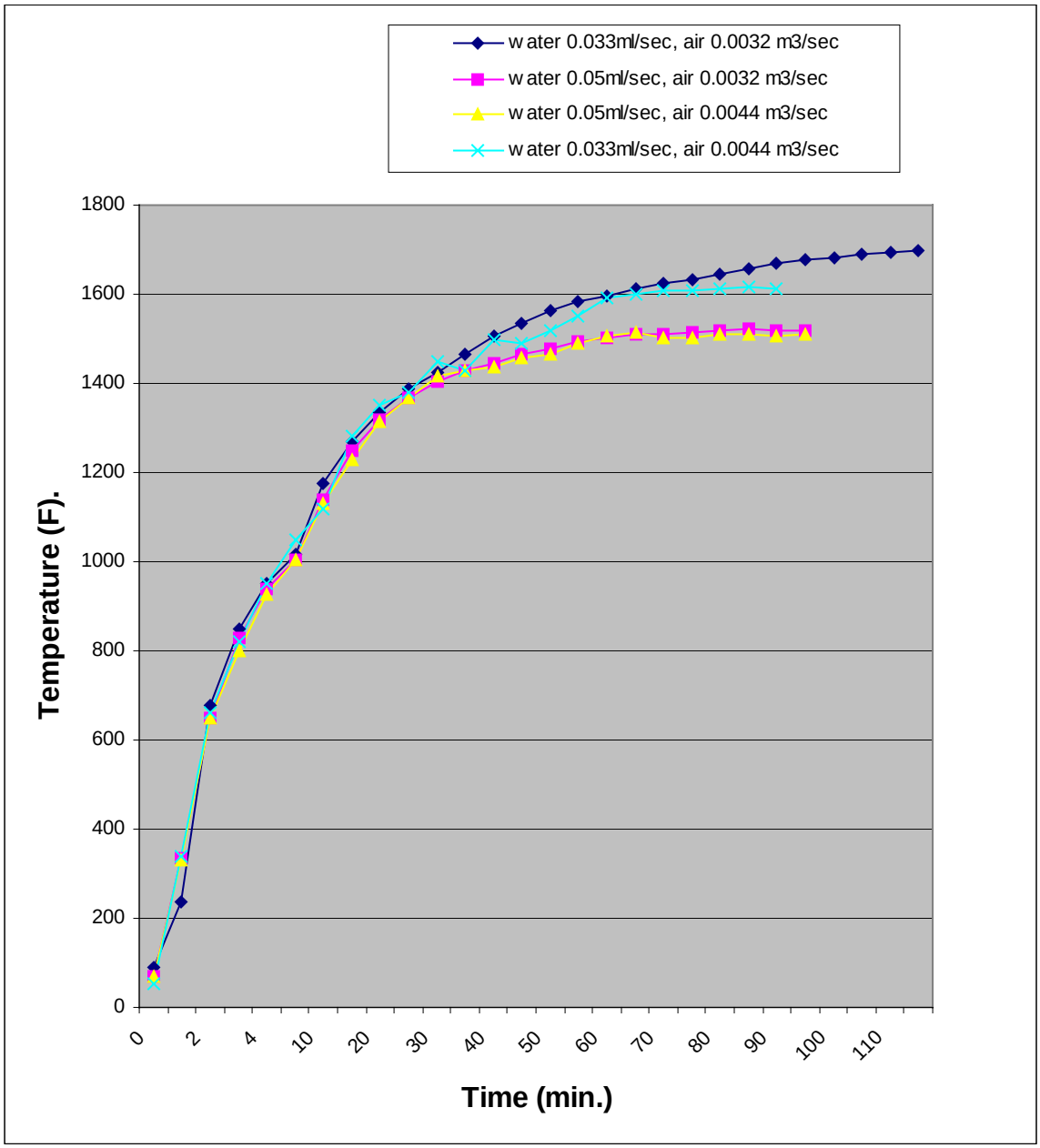

Figure 14. Temperature Heating Up Curve with Water and Air Injections

Comparing the four cases shown in Table 5, the water injection rate was the significant factor to the temperature heating up rate and steady state temperature. When the water injection rate increased from 2 ml/minute to 3 ml/minute, the steady state temperatures were reached at 65 minutes, and 105 minutes, respectively. The steady state temperatures for these four cases varied from 1505 to 1650 F.

After the steady state condition was reached (The steady state condition is defined as the condition when the temperature change is less than 5 F within 5 minutes period), three temperature readings were selected for each of these four (4) cases.

From the Analysis of Variance (ANOVA) Table 6, at the 95% confidence and 0.9996 of R-squared, the air injection rate was the significant factor on the temperature. The water injection rate was not significant as comparing to air injection rate.

Table 6. ANOVA Table for Temperature Changes (First Temperature Reading)

Number of obs	= 4	R-squared	=	0.9996	
Root MSE	= 2	Adj R-squared	=	0.9989	
Source	Partial SS	df	MS	F	Prob > F
Model	11285	2	5642.5	1410.63	0.0188
Water injection rate	49	1	49	12.25	0.1772
Air injection rate	11236	1	11236	2809.00	0.0120
Residual	4	1	4		
Total	11289	3	3763		

From the ANOVA Table 7, at the 95% confidence and 0.9983 of R-squared, the air injection rate was the significant factor on the temperature (since the air probability is 0.0266<0.05). The water injection rate was not significant as comparing to air injection rate.

Table 7. ANOVA Table for Temperature Changes (Second Temperature Reading)

Number of obs	= 4	R-squared	=	0.9983	
Root MSE	= 4.5	Adj R-squared	=	0.9948	
Source	Partial SS	df	MS	F	Prob > F
Model	11688.5	2	5844.25	288.60	0.0416
Water injection rate	132.25	1	132.25	6.53	0.2375
Air injection rate	11556.25	1	11556.25	570.68	0.0266
Residual	20.25	1	20.25		
Total	11708.75	3	3902.91667		

From the ANOVA Table 8, at the 88% confidence and 0.9716 of R-square, the air injection rate was the significant factor on the temperature.

Table 8. ANOVA Table for Temperature Changes (Third Temperature Reading)

Number of obs	= 4	R-squared	=	0.9716	
Root MSE	= 22.5	Adj R-squared	=	0.9148	
Source	Partial SS	df	MS	F	Prob > F
Model	17312.5	2	8656.25	17.10	0.1686
Water injection rate	1056.25	1	1056.25	2.09	0.3855
Air injection rate	16256.25	1	16256.25	32.11	0.1112
Residual	506.25	1	506.25		
Total	17818.75	3	5939.58333		

4.2 Feasibility Test Results and Analysis of Thermocouple Vibration

The detailed experimental facility setup and procedures are shown in the previous section 3.2.3. The experimental data of this test is shown in Table 3. The ANOVA table based on the experimental data was calculated for each set of data to determine whether the vibration affected the temperature measurement. Table 9 shows the ANOVA analysis on data set 1 (temperature reading 1) shown in Table 3, Table 10 shows the ANOVA analysis on data set 2 (temperature reading 2) in Table 3, and Table 11 shows the ANOVA analysis on data set 3 (temperature reading 3) also shown in Table 3.

Table 9. ANOVA Table for Temperature Reading 1

Number of obs	=	4	R-squared	=	1.0000
Root MSE	=	10.55	Adj R-squared	=	0.9999

Source	Partial SS	df	MS	F	Prob > F
Model	2861788.92	2	1430894.46	12855.91	0.0062
Motor speed	109.202516	1	109.202516	0.98	0.5030
Temp. level	2861679.71	1	2861679.71	25710.83	0.0040
Residual	111.302484	1	111.302484		
Total	2861900.22	3	953966.74		

Table 10. ANOVA Table for Temperature Reading 2

Number of obs	=	4	R-squared	=	1.0000
Root MSE	=	0.1	Adj R-squared	=	1.0000

Source	Partial SS	df	MS	F	Prob > F
Model	2965628.41	2	1482814.21		
Motor speed	.009999695	1	.009999695	1.00	0.5000
Temp. level	2965628.4	1	2965628.4		
Residual	.009999695	1	.009999695		
Total	2965628.42	3	988542.808		

Table 11. ANOVA Table for Temperature Reading 3

Number of obs	=	4	R-squared	=	1.0000
Root MSE	=	10.95	Adj R-squared	=	0.9999

Source	Partial SS	df	MS	F	Prob > F
Model	2785516.21	2	1392758.1	11615.75	0.0066
Motor speed	122.102483	1	122.102483	1.02	0.4971
Temp. level	2785394.11	1	2785394.11	23230.49	0.0042
Residual	119.902517	1	119.902517		
Total	2785636.11	3	928545.37		

Table 12 shows the ANOVA analysis for temperature in the above three conditions replication that includes the motor and temperature level interaction.

Table 12. ANOVA Table for Temperature Readings 1-3

Number of obs	=	12	R-squared	=	0.9997
Root MSE	=	19.3156	Adj R-squared	=	0.9995

Source	Partial SS	df	MS	F	Prob > F
Model	8611587.93	3	2870529.31	7693.90	0.0000
Motor speed	155.519978	1	155.519978	0.42	0.5366
Temp. level	8611279.75	1	8611279.75	23080.87	0.0000
Speed*level	152.653355	1	152.653355	0.41	0.5403
Residual	2984.73333	8	373.091666		
Total	8614572.66	11	783142.969		

From Tables 9-12, it can be seen that the thermocouple vibration did not have the significant impact to the temperature measurements in the gasifer simulator regardless of the temperature levels. The interaction between the motor speed and temperature level was not significant, either. Based on the results, the thermocouple vibration did not have the significant impact to the temperature measurements in the gasifier simulator.

4.3 Sub-Sonic Thermocouple Vibration Tests Results and Analysis

The detailed experimental facility setup and procedures are shown in the previous section 3.2.4. The ANOVA analysis shown in Table 13 was used to determine whether the vibration frequency or vibration amplitude affected the removal performance on the concrete cover layer. This ANOVA was conducted based on the data shown in Table 4. Table 13 shows the ANOVA analysis on the results and analysis of the sub-sonic thermocouple vibration tests.

Table 13. The ANOVA Analysis Results of the Sub-sonic Thermocouple Vibration Tests

Number of obs =	9	R-squared =	0.8663		
Root MSE	= .039619	Adj R-squared =	0.6658		
Source	Partial SS	df	MS	F	Prob > F
Model	.020345305	3	.006781768	4.32	0.1937
v	.018161002	1	.018161002	11.57	0.02766
h	.002184304	2	.001092152	0.70	0.05589
Residual	.003139303	2	.001569652		
Total	.023484609	5	.004696922		

v: vibration; h: frequency

From Table 13, the ANOVA results show that the vibration amplitudes did have the significant impact to the concrete cover layer elimination process. The vibration frequency did also have the significant impact to the concrete cover layer removal process. In addition, the results show that the amplitude had more significant impacts to the concrete cover layer elimination than frequency.

5. CONCLUSIONS

The major accomplishments in this semi-annual period are listed below.

1. The systematic tests in the gasifier simulator are being successfully conducted during this reporting period.
2. ANOVA analysis is a very effective method to analyze the complicated experimental system and data.
3. Water injection rate did not have the significant impact on the temperature measurements in the gasifier simulator, which proved the moisture immunity of the proposed temperature measurement device.
4. The air injection rate did have the significant impact on the temperature measurement in the gasifier simulator.
5. The specially designed water introducing system could successfully feed small amount of water into the gasifier simulator to create the moisturized environment.
6. The high-speed electric motor can be used to create the thermocouple vibration within the sub-sonic frequencies using unbalanced object at the motor shaft.
7. The sub-sonic vibration could reduce the weight of the solid concrete cover layer on the thermocouple tip. The continuing research efforts are expected to provide more information in the future.
8. The sub-sonic vibration frequency and amplitude are believed to have significant impacts to the concrete cover layer elimination process.

RESEARCH CONTINUATION

The progress of this project has been on schedule. The natural frequency of the concrete cover layer will be determined during April 2004. The systematic tests will be continued in the gasifier simulator (hot model) with more operation parameters (Air purging frequencies and powder amount in the gasifier simulator). The ultrasonic cleaning application for the gasifier simulator (hot model) will be applied to the thermocouple assembly.

REFERENCES

1. Williams, A., M. Pourkashanian, N. Skorupska, Combustion and Gasification of Coal, Taylor & Francis; ISBN: 1560325496, May 2000.
2. Edgar, Thomas F., Coal Process and Pollution Control, Gulf Publish Company, 1983.
3. Montgomery, D. C., Design and Analysis of Experiments, 4th Edition, 1997.
4. Anderson, Mark J., Patrick J. Whitcomb, An Introduction to Design of Experiments: A Simplified Approach, American Society for Quality; ISBN: 0873894448, January 1999.
5. Lee, S. W., "Innovative Instrumentation and Analysis of the Temperature Measurement for High Temperature Gasification" DOE Progress Report II, October 2003.
6. Lee, S. W., "Innovative Instrumentation and Analysis of the Temperature Measurement for High Temperature Gasification" DOE Progress Report I, April 2003.
7. Gexue, R., L. Qiuhai, H. Ning, N. Rendong, and N. Bo, On Vibration Control with Stewart Parallel Mechanism, Mechatronics, Feb 2004.
8. Antoni, J. and R.B. Randall, Unsupervised Noise Cancellation for Vibration Signals: Part I - Evaluation of Adaptive Algorithms, Mechanical Systems and Signal Processing, Jan 2004.
9. Tsujino, J. K. Hidai, A. Hasegawa, R. Kanai, H. Matsuura, K. Matsushima, T. Ueoka, Ultrasonic Butt Welding of Aluminum, Aluminum Alloy and Stainless Steel Plate Specimens, Ultrasonics, May 2002.
10. Ku, H.S., F. Siu, E. Siores, J.A.R. Ball, Variable Frequency Microwave (VFM) Processing Facilities and Application in Processing Thermoplastic Matrix Composites, Journal of Materials Processing Technology, Aug 2003.
11. Hadavinia, H., A. J. Kinloch, M. Little, A. Taylor, The Prediction of Crack Growth in Bonded Joints under Cyclic-fatigue Loading I. Experimental Studies, International Journal of Adhesion and Adhesives, Jan 2003.
12. Wu, Jia-Jang, Vibration of a Rectangular Plate Undergoing Forces Moving Along a Circular Path, Finite Elements in Analysis and Design, Nov 2003.
13. Xiang, Y., J. N. Reddy, Natural Vibration of Rectangular Plates with an Internal Line Hinge Using the First Order Shear Deformation Plate, Journal of Sound and Vibration, May 2003.